

SCIENTIFIC REPORTS



OPEN

Mediterranean versus Red sea corals facing climate change, a transcriptome analysis

Keren Maor-Landaw¹, Hiba Waldman Ben-Asher¹, Sarit Karako-Lampert¹, Mali Salmon-Divon², Fiorella Prada³, Erik Caroselli³, Stefano Goffredo³, Giuseppe Falini⁴, Zvy Dubinsky¹ & Oren Levy¹

Received: 04 August 2016

Accepted: 09 January 2017

Published: 09 February 2017

The anthropogenic increase in atmospheric CO₂ that drives global warming and ocean acidification raises serious concerns regarding the future of corals, the main carbonate biomineralizers. Here we used transcriptome analysis to study the effect of long-term gradual temperature increase (annual rate), combined with lowered pH values, on a sub-tropical Red Sea coral, *Stylophora pistillata*, and on a temperate Mediterranean symbiotic coral *Balanophyllia europaea*. The gene expression profiles revealed a strong effect of both temperature increase and pH decrease implying for synergism response. The temperate coral, exposed to a twice as high range of seasonal temperature fluctuations than the Red Sea species, faced stress more effectively. The compensatory strategy for coping apparently involves deviating cellular resources into a massive up-regulation of genes in general, and specifically of genes involved in the generation of metabolic energy. Our results imply that sub-lethal, prolonged exposure to stress can stimulate evolutionary increase in stress resilience.

Corals worldwide have been affected by global warming and the accompanying ocean acidification, experiencing reduced skeleton calcification and severe bleaching events that often lead to coral death^{1,2}. The Mediterranean sea is considered a “biodiversity hotspot”³, but is particularly sensitive to climate change^{4,5} and to ocean acidification⁶. Mediterranean corals thrive despite a wide annual fluctuation of sea surface temperatures (SSTs), ranging ~13 °C in the Ligurian Sea, compared to sub-tropical corals, facing only a ~6 °C fluctuation in the Red Sea⁷. This demonstrates the adaptability of some scleractinian corals and suggests that understanding the compensatory cellular mechanism of temperate corals is crucial to forecast the overall fate of corals in an era of global warming and ocean acidification.

The effects of global change on corals have been the subject of intensive research in the last decades, but have mainly focused on tropical corals. Here for the first time, we subject a sub-tropical Red Sea coral and a temperate coral from the Mediterranean, to a slow, chronic temperature increase (mimicking the annual rate), together with the low pH values (7.8) expected by the end of the century¹ in a long-term experiment and analyze the response by ‘in silico’ high-throughput sequencing techniques, aligned with bioinformatics and physiological tools.

The sub-tropical *Stylophora pistillata* (Esper, 1797), a robust⁸, r strategist⁹, scleractinian symbiotic colonial branching, hermatypic coral (Fig. 1C), found across the Indo-Pacific, is a well-studied ‘guinea pig’ coral¹⁰. The temperate *Balanophyllia europaea* (Risso, 1826), a complex⁸, scleractinian symbiotic solitary oval shaped coral (Fig. 1D), inhabits Mediterranean rocky foreshores to a depth of 50 meters, with dozens of polyps per square meter¹¹. Reduced skeletal calcification¹², higher skeletal porosity¹³ and lower population densities¹⁴ have been reported with increased seawater temperature and ocean acidification^{15,16}. To date there are no available genomic nor transcriptomic data available on Mediterranean corals, including on *B. europaea*¹⁷, whereas an ESTs library was previously constructed for *S. pistillata*¹⁸.

¹The Mina and Everard Goodman Faculty of Life Sciences, Bar Ilan University, Ramat Gan, Israel. ²Department of Molecular Biology, Ariel University, Ariel, Israel. ³Marine Science Group, Department of Biological, Geological and Environmental Sciences, Section of Biology, Alma Mater Studiorum–University of Bologna, Bologna, Italy. ⁴Dipartimento di Chimica ‘G. Ciamician’, Alma Mater Studiorum Università di Bologna, Bologna, Italy. Correspondence and requests for materials should be addressed to S.G. (email: s.goffredo@unibo.it) or O.L. (email: oren.levy@biu.ac.il)

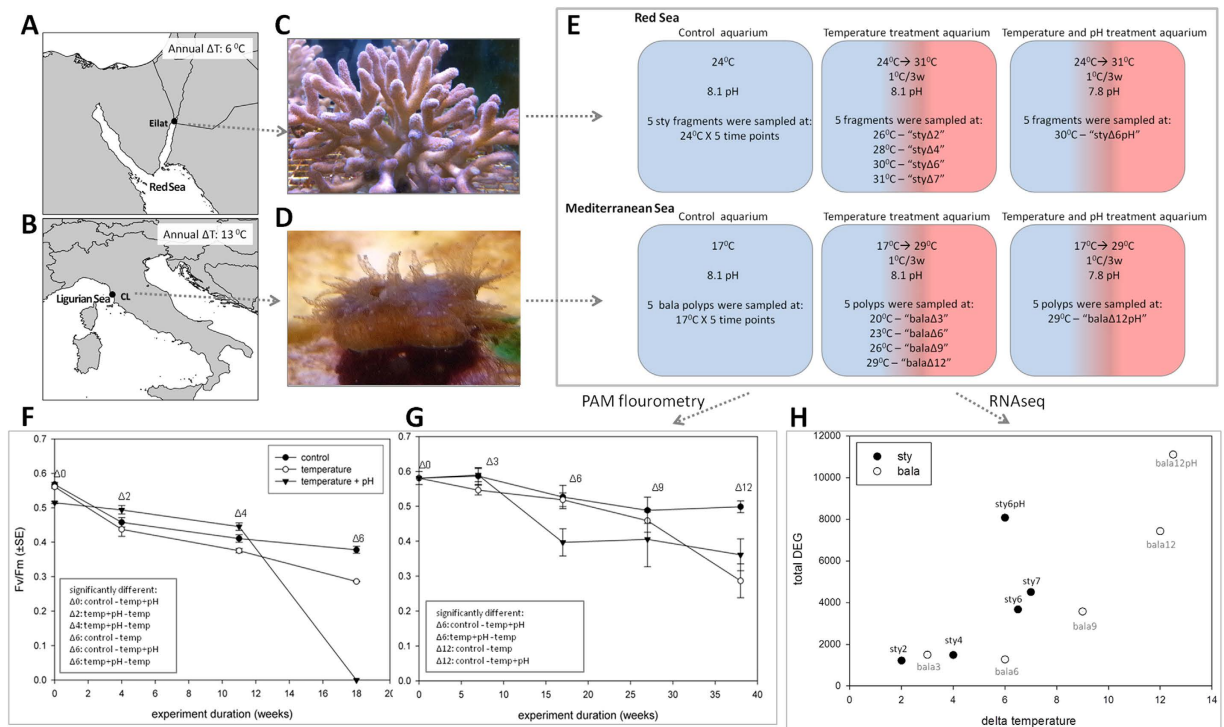


Figure 1. Experimental design, algal maximum quantum yield and numbers of differentially expressed genes. (A,B) Sampling locations (Calafuria; CL, Ligurian Sea and Eilat, Red Sea) and their annual delta temperatures. (Made with Natural Earth. Free vector and raster map data @ www.naturalearthdata.com. QGIS Development Team, 2016. QGIS Geographic Information System. Open Source Geospatial Foundation Project. <http://www.qgis.org>) (C) A colony of *S. pistillata* (sty). (D) A polyp of *B. europaea* (bala). (E) Experimental design. (F,G) Algal maximum quantum yield (Fv/Fm) in *S. pistillata* fragments and *B. europaea* polyps, respectively. The numbers shown in the data labels represent the delta temperatures compared to the control in the treatment aquaria. The tables in the left lower corner contain significant differences by one-way ANOVA and post-hoc LSD multiple comparison test ($p < 0.05$). (H) Differentially expressed genes (DEGs) in *S. pistillata* and *B. europaea* by treatment.

Our work on the thermotolerant Mediterranean coral *B. europaea* in comparison to *S. pistillata* contributes to the understanding of how prolonged exposure to sub-lethal stress directs the evolutionary increase in stress resilience.

Results and Discussion

S. pistillata colonies from the Gulf of Aqaba, Red Sea, and *B. europaea* polyps from Calafuria, Ligurian Sea, north of Italy (Fig. 1A,B), were allocated to Red Sea or Mediterranean conditions, each habitat type comprised three treatments: (1) control with ambient conditions (2) temperature +1 °C increase every three weeks (3) temperature and pH-pH 7.8 with 1 °C increase every three weeks (Fig. 1E). Experimental duration was eight and five months according to the natural SST inclination for the Mediterranean and Red Sea corals, respectively. Coral samples were collected at intervals for RNA extraction and the maximum quantum yield (Fv/Fm) of algal symbionts was calculated as a measure of photosynthetic performance, which is considered as an indicator of thermal stress^{19–21}.

For *B. europaea*, Fv/Fm (algal maximum quantum yield) values were higher than those for *S. pistillata*, most notably at the combined treatment of 7.8 pH and 6 °C elevation in comparison to the control (Fig. 1G). This reflects the lower annual change in SST of the sub-tropical habitat (Fig. 1A,B inset), placing *S. pistillata* as sensitive to heat stress and lower pH in comparison to *B. europaea* (Fig. 1F). Significant change was observed between the temperature and the integrated temperature-pH treatments in some measuring points, implying on a synergistic effect between pH and temperature.

S. pistillata and *B. europaea* sequenced reads were assembled into transcriptomes of 159,679 and 313,813 open-reading-frame-contigs, respectively and fold changes were calculated for all contigs. Differentially expressed genes (DEGs) were arbitrarily defined as those exceeding a two-fold-change (p -value < 0.05). The first increase in DEGs (Fig. 1H) was seen in *S. pistillata* at 6 °C above control (sty6), but only after 9 °C (bala9) in *B. europaea*. However, in both corals DEG numbers increased with temperature and even more with combined temperature-pH, although the ratio of up- vs. down-regulated genes, showed species differences (Table 1). In *S. pistillata* the percentage of up- and down-regulated genes were similar throughout most of the experiment, but in *B. europaea* the percent of down-regulated genes increased from 3% of total DEGs at the beginning, to 43% by the end of the experiment. With combined temperature-pH treatment, most (71%) of the DEGs

<i>S. pistillata</i>	Total DEGs	% ↓	<i>B. europaea</i>	Total DEGs	% ↓
2	1219	44.9	3	1495	2.9
4	1487	37.9	6	1274	7.0
6	3668	53.1	9	3572	19.8
7	4504	58.3	12	7425	42.3
6 pH	8072	71.1	12 pH	11102	43.6

Table 1. Percentage of down-regulated genes out of total differentially expressed genes (DEG) in *S. pistillata* and *B. europaea* treatments (2, 4, 6, 7 and 3, 6, 9, 12; temperature elevation above the control of *S. pistillata* and *B. europaea*, respectively, and pH7.8).

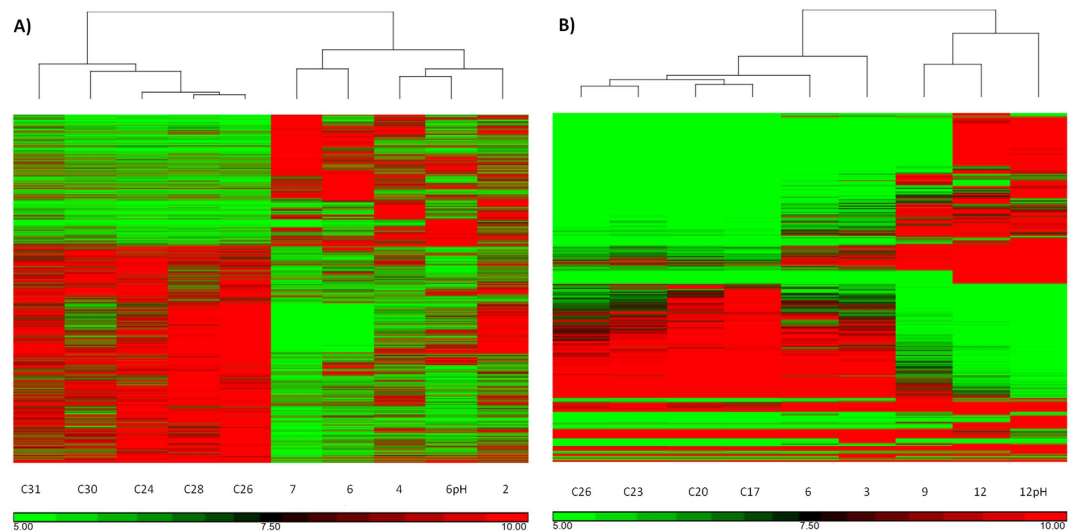


Figure 2. Heat maps of hierarchical clustering of *S. pistillata* (A) and *B. europaea* (B) samples. 2, 4, 6, 7, 6 pH and 3, 6, 9, 12, 12 pH, stand for the delta in temperature compared to the control, in *S. pistillata* and *B. europaea*, respectively. The Cs stand for the control samples (*S. pistillata*–24 °C, *B. europaea*–17 °C) and the number that follows represents the aquarium temperature at the time point.

were down-regulated in *S. pistillata* but not in *B. europaea*. The clustering in control samples can be seen in three-dimensional space principle components (PC) (Fig. S1) and hierarchical clustering heat maps (Fig. 2). An elevation of only 2 °C was sufficient to change the pattern of gene expression in *S. pistillata* but at least an increase of 9 °C was needed to separate *B. europaea* from the control.

A model summarizing selected Gene Ontologies (GO) and pathways in *S. pistillata* and *B. europaea* over the course of the experiment shows the up/down regulated cellular processes and implies different cellular responses to stress (Fig. 3). GOs enriched early in *S. pistillata*, including protein ubiquitination and apoptosis, appear only later in the experiment in *B. europaea*. GOs that are related to cell morphological changes could be a manifestation of this heat stress in *S. pistillata*. In contrast, ribosome biogenesis, generation of precursor metabolism and energy, and intracellular transport processes, appear earlier in *B. europaea* than *S. pistillata*, while the process of carbohydrate catabolism is absent from *S. pistillata*. We postulate that the enrichment of metabolic processes (generation of precursor metabolism and energy and cellular carbohydrate catabolic process) might enable *B. europaea* to postpone temperature-induced protein degradation and cell death.

Enrichment analyses of the specifically temperature-pH DEGs were generated for each coral species (see in Fig. S5 Venn diagram the 5,984 and 4,857 unique temperature-pH genes of *S. pistillata* and *B. europaea*, respectively) and compared to the matching temperature treatment (unique sty6pH to sty6 and unique bala12pH to bala12) (Tables S4 and S5). This analysis revealed that as expected^{22,23}, transport processes were modified by temperature and pH in both corals, but in *S. pistillata* there was an effect on protein degradation while the response to stress in *B. europaea* involved metabolic processes.

Thirty-nine DEGs, identified from the KEGG database as being associated with the adherens junction (AJ) pathways and regulation of actin cytoskeleton were enriched in *S. pistillata* at +2 °C and in *B. europaea* at +6 °C (Fig. 4). Interestingly, detachment of endoderm cell containing *Symbiodinium* is one of the proposed mechanisms of coral bleaching²⁴. A combination of 30 °C and pH7.8 down regulated *S. pistillata* β -catenin and δ -catenin as well as cadherin, weakening cell-cell adhesion and facilitating coral bleaching²⁵. In contrast, at +6 °C the cadherin-catenin positive regulator casein kinase II (CKII) as well as other AJ elements were up-regulated in *B. europaea* (Fig. 4) with increased temperature and pH.

ScanProsite²⁶ domain-prediction analysis of “extreme” DEGs, (changing at least ten fold) revealed an enrichment of proteins (Fisher’s exact test, 2-tail $p < 0.05$) containing the conserved BRICHOS domain²⁷ in *S. pistillata*;

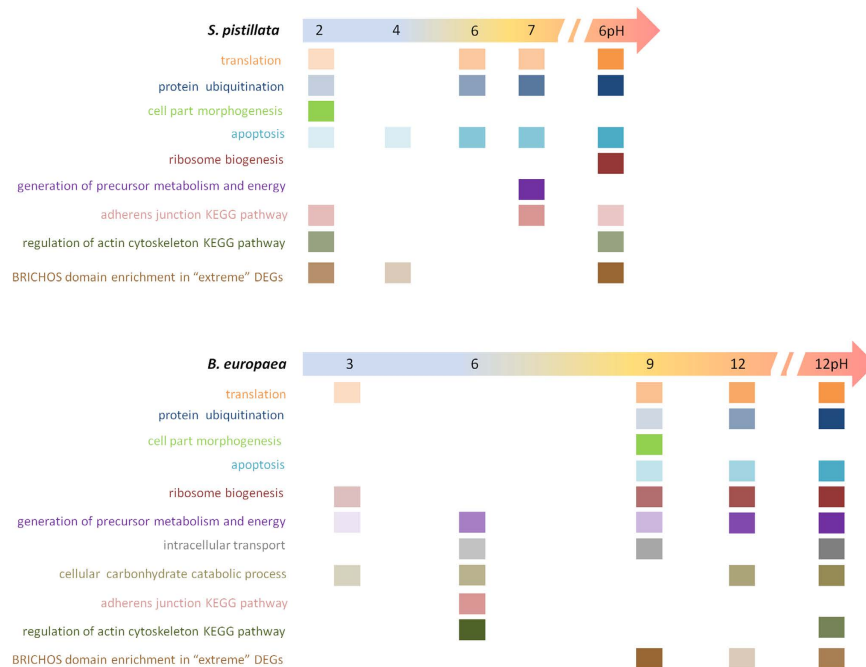


Figure 3. A model summarizing enriched cellular processes in *S. pistillata* and *B. europaea* throughout the experiment. The categories on the left are based on Gene Ontologies and KEGG pathways retrieved David or STRING databases. Treatments giving BRICHOS domain enrichment in “extreme” (at least ten fold change) DEGs. 2, 4, 6, 6 pH, 7 and 3, 6, 9, 12, 12 pH indicate the delta of temperature compared to the control, in *S. pistillata* (sty) and *B. europaea* (bala), respectively. The color intensity gradient of the squares represents the enrichment of the treatment with the GO/pathway.

+2 °C, +4 °C and especially at +6 °C-pH (up to 380 fold increase), and in *B. europaea* at; +9 °C, +12 °C and +12 °C-pH (Fig. 3). Crystal structure²⁷ and functional mutation²⁸ studies strongly imply that BRICHOS domain is acting as a chaperone. BRICHOS domain was uncovered in a hydrothermal worm and was hypothesized to contribute to the worm’s evolution-driven unique adaptation to survive under extreme conditions²⁹. Clustal Omega alignment³⁰ of 238 BRICHOS domain sequences retrieved from 15 coral species transcriptome databases) (<http://comparative.reefgenomics.org/datasets.html>)¹⁷ using ScanProsite²⁶ (Fig. S7), revealed that corals shared the overall conserved BRICHOS architecture³¹ including the pair of cysteine residues (positions 30 and 105) that probably form a disulfide bridge³¹. Moreover, some residues were specific for corals (for example A in position 7, G-81, N-98). At the present stage we can only speculate whether proteins possessing this domain could play a major role as unique chaperones or fulfill some other yet unknown novel function in the coral response to environmental stress.

This study demonstrates that temperate corals used to higher annual temperature fluctuations than those faced by tropical species, have developed thermotolerance and resistance to pH change. It has been previously shown that daily environmental fluctuations in a physically challenging microhabitat promote thermotolerance in corals^{32–34}. Our results are also in agreement with the concepts developed by Nevo³⁵, showing, that sub-lethal, prolonged exposure to any stress can stimulate genetic polymorphism and the resulting evolutionary increase in stress resilience. A recent work by Hume *et al.*³⁶ argue that positive selection can facilitate adjustment to temperature extremes of coral symbionts in the Persian/Arabic Gulf which endorses these concepts as well.

A deeper understanding of the genomic plasticity across latitudes and marine ecological niches may improve our projections of the ‘winners and losers’ and the future of coral ecosystems under the threat of global change.

Material and Methods

Coral collection and maintenance. *Balanophyllia europaea* polyps were collected from Calafuria, in the Ligurian Sea, north of Italy, shipped to Bar-Ilan University, Israel, and placed into an aquarium maintained at 17 °C for several months prior to the experiment. *Stylophora pistillata* colonies were collected while SCUBA diving at a depth of 10 m in the Gulf of Aqaba, Eilat (Red Sea) and maintained at 24 °C at Bar-Ilan University, Israel.

All the corals were acclimated and maintained in 600 L aquariums with circulating artificial seawater (Brightwell Aquatics) under controlled constant conditions of temperature and 35‰ salinity, mimicking the average annual ambient temperatures conditions. The annual cycle of diurnal-dimming light regime was simulated with an Advanced Control Lighting System (ACLS, Sfiligoi, Italy) and HQI (Hydrargyrum quartz iodide) light bulbs (400 W, 14000 Kelvin). The corals were fed once a day with a microvore microdiet (Brightwell Aquatics). Following the acclimation period, the corals were transferred into 300 L aquariums, with the running flow controlled by a computer system, through closed circulation to compensate for salinity fluctuations and water level changes (constant salinity level of 35‰).

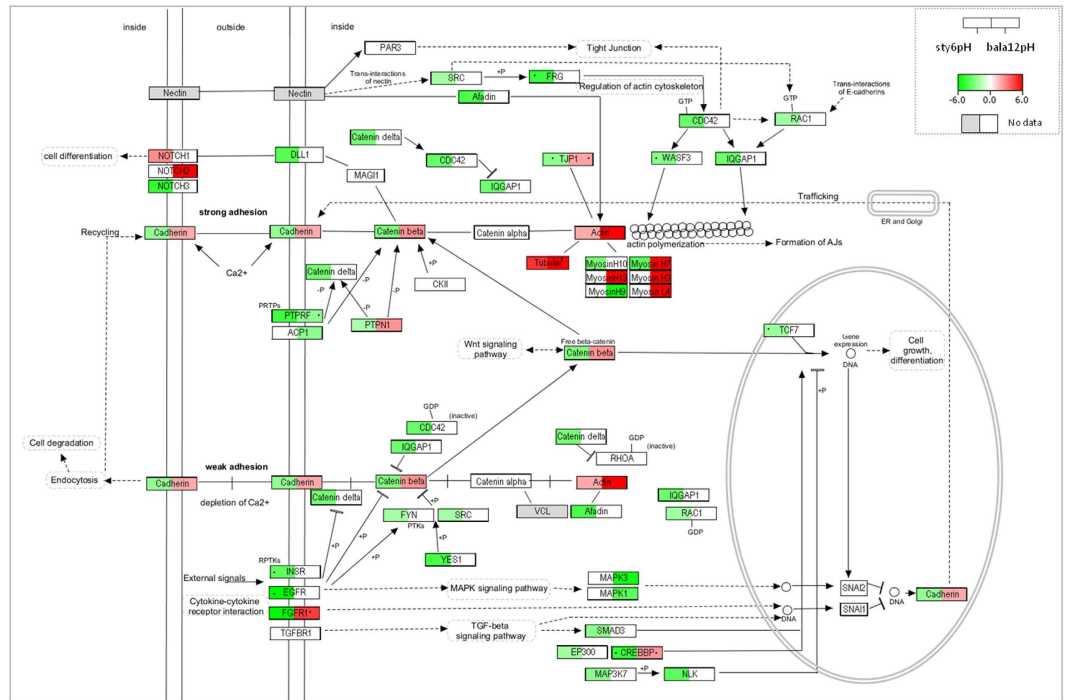


Figure 4. Adherens junction (AJ) pathway and *S. pistillata* +6°C-pH (sty6pH) and *B. europaea* +12°C-pH (bala12pH) fold changes. Fold changes of sty6pH (left) and bala12pH (right) genes are represented by a color scale. A dot stands for an insignificant contig annotation corresponding to each organism and ref. 1 for an average fold change value of several contig annotations. AJs are mediated through calcium-dependent cadherins linked to the actin cytoskeleton via α - and β -catenins⁴⁹. Chordate-like classic cadherins were not observed in the cnidarian *Nematostella*⁴⁹, as well as in our studied corals, however, the cadherin genes found belong to the protocadherin subfamily of cadherin superfamily. Regulation of AJs can be by α -catenin interactions with actin-associated proteins (Afadin and VCL), via the small GTPase RAC1 and Cdc42⁵⁰, or alternatively through posttranslational modifications of AJ components. Cadherin-catenin complexes are negatively regulated by tyrosine phosphorylation of β -catenin by receptor tyrosine kinases or cytoplasmic tyrosine kinases; SRC, Fyn and YES1 and positively regulated by casein kinase II (CKII) and protein tyrosine phosphatases (PTPs). Additional regulation is through GTPase-activating protein IQGAP binding to RAC1, which is thought to displace the latter from interacting with β -catenin, thereby freeing β -catenin to interact with α -catenin. Dissociation of β -catenin is likely to render cadherin susceptible to proteasome-mediated degradation or recycling back to the cell surface⁵⁰. WNT signaling acts as a positive regulator, activating transcription factors by stabilizing β -catenin and promoting its binding to TCF (transcription factor3). Various growth factors, including: HGF, FGF, and TGF β 2, regulate cadherin expression indirectly via transcription factor SNAI2/Slug, which eventually inhibits cadherin expression. Transcriptional activation of β -catenin is stimulated via TGF-beta signaling by enhancing the interaction between CREBB-binding protein and SMAD⁵¹. Adhesion of neighboring cells can also be mediated via NOTCH and DLL1 or nectin, which results in lateral inhibition of cell differentiation and firm adhesion.

Experimental design. For the Red Sea coral experiments, six *S. pistillata* colonies were placed in each 300 L aquarium: (1) Control aquarium—constant 24°C (mimicking the average annual ambient temperatures conditions) and ambient pH. (2) Temperature treatment—Increase in temperature from 24°C to 31°C at a rate of 1°C every three weeks (mimicking the annual rate in Eilat) under ambient pH. (3) Temperature and pH treatment—1°C increase every three weeks from 24°C to 31°C while maintaining a pH of 7.8. Two fragments approximately 2 cm long were chopped and sampled from the upper branches of every colony and aquarium, at the beginning of the experiment and a week after the temperatures reached: 26°C, 28°C, 30°C, and 31°C.

For the Mediterranean coral experiments, *B. europaea* polyps were placed in each of three aquaria: (1) Control aquarium - constant 17°C (mimicking the average annual ambient temperatures conditions) and ambient pH. (2) Temperature treatment—Increase in temperature from 17°C to 29°C at a rate of 1°C increase every three weeks under ambient pH. (3) Temperature and pH treatment—1°C increase every three weeks from 17°C to 29°C while maintaining a pH of 7.8. Five polyps from every aquarium were sampled, at the beginning of the experiment at 17°C and then a week after the temperatures reached: 20°C, 23°C, 26°C and 29°C. The sampled fragments and polyps were snap-frozen in liquid nitrogen and kept at -80°C for RNA extraction.

PAM fluorometer. A MAXI imaging Pulse Amplitude Modulation (iPAM) fluorometer (Heinz Waltz GmbH, Germany) was used to evaluate the maximum quantum yield of photosystem II of the algal symbionts

of Red Sea *S. pistillata* and Mediterranean *B. europaea*. Following 30 min of dark adaptation, triplicate measurements of the fluorescence in each aquarium were taken at each time point.

RNA extractions. RNA was extracted from *B. europaea* polyps using Total RNA kit (A&A Biotechnology), according to manufacturer's instructions, with the minor modifications that all the centrifugations were cooled and the RNA was extracted using double the recommended amount of Fenzol (in order to cover the entire fragment), and was vortexed during the 5 minute incubation. Following the incubation, the tube was centrifuged 12,000 g, 20 min, in order to reduce algae cell contamination and remove the remains of the unwanted pellet. The final elution volume was 50 μ l.

Total RNA was extracted from *S. pistillata* fragments using Trizol (Invitrogen Life Technologies, Carlsbad, CA, USA) according to the methods previously described³⁷.

The concentration of the RNA was measured using a NanoDrop spectrophotometer (ND-1000), and the quality (RIN number >8.5) assessed by a Bioanalyzer (Agilent).

Transcriptome sequencing, library preparation and assembly. Samples of total RNA from *S. pistillata* and *B. europaea* were pooled (into 1 μ g each sample) and sent to the IGA Technology Services facility in Udine, Italy for pair-end Hiseq barcoding. Upon arrival at the IGA total RNA of the samples was re-analyzed with an Agilent 2100 Bioanalyzer system (Agilent, Waltham, MA) to ensure that no damage had occurred during shipment. Libraries were prepared using the 'TruSeq mRNA Sample Prep kit' (Illumina, San Diego, CA) according to the manufacturer's instructions. Poly-A mRNA was fragmented (3 min at 94 °C) and every purification step was performed using 1X Agencourt AMPure XP beads.

The final libraries were quantified by using a Qubit 2.0 Fluorometer (Invitrogen, Carlsbad, CA) and quality tested by Agilent 2100 Bioanalyzer High Sensitivity or DNA 1000 assay (Agilent Technologies, Santa Clara, CA). Libraries were then processed with Illumina cBot for cluster generation on the flowcell and sequenced in paired-end mode on HiSeq2500 (Illumina, San Diego, CA), following the manufacturers' instructions for a rapid run. The CASAVA 1.8.2 version of the Illumina pipeline was used to process raw data for both format conversion and de-multiplexing. The Fastq files have been deposited at SRA database under the accessions: SRP075606 (*Balanophyllia europaea*) and SRP075598 (*Stylophora pistillata*).

Pooled sequences from the 20 sampled treatments were used (10 for each coral) to assemble the *S. pistillata* and the *B. europaea* transcriptomes. Trim Galore software (www.bioinformatics.babraham.ac.uk/projects/trim_galore/) was used for trimmed off sequencing adapters, low quality reads and for quality control. The reads were submitted to Trinity software (version r20131110)³⁸ for *de novo* assembly using the default parameters. *S. pistillata* and *B. europaea* library assemblies resulted with 470,497 and 961,667 contigs (transcripts), respectively. Each set of reads from each sample was then aligned to the assembled transcriptome using Bowtie, and RSEM³⁹ was next applied in order to get sample-specific abundance estimates. The last two steps were done using the "run_RSEM_align_n_estimate.pl" script from the Trinity software package using the default parameters. In order to minimize false positive isoforms, all transcripts having FPKM value <1 or isoform percentage values (IsoPct%) <1 were filtered out, and were not included in downstream analysis. 162,784 contigs (N50 = 2088, median contig length = 687) and 546,169 contigs (N50 = 1246, median contig length = 424) were left after filtering in *S. pistillata* and *B. europaea* assemblies respectively. Putative coding regions were extracted from the transcriptome assemblies using TransDecoder software (www.transdecoder.sourceforge.net), providing all the CDS and proteins from the assembly. The *S. pistillata* library contained 159,679 open reading frame (ORF)-encoding contigs and the *B. europaea*, 313,813. From which 71,096 and 213,664 protein coding genes are for *S. pistillata* and *B. europaea*, respectively. Bowtie (v2.1.0) was again used to map each set of reads from each sample against CDS, FPKM was calculated for expression values.

Annotations were created by blasting the proteome against the *Homo sapiens* database using BLASTP (NCBI). Annotations were also created from the Swissprot and Uniprot50 databases by BLASTP. We applied filtering to the BLASTP results in order to increase the certainty of obtaining true homologs. With regards to the *H. sapiens* annotations, our filtering parameters were set at an e-value threshold of 5×10^{-5} , >30% alignment identity and >70% query coverage. After annotation filtration, 22,881 annotated contigs remained for *S. pistillata* and 61,908 contigs for *B. europaea*.

Validation using quantitative real-time PCR. To validate the RNA-seq results, quantitative real-time polymerase chain reaction (qRT-qPCR) assays were performed for four highly expressed selected genes and a comparison made between the results in the treated and control samples. For *S. pistillata*, small heat shock protein and calmodulin genes, which were up- and down-regulated respectively, after 30 °C treatment, were selected. For *B. europaea*, we selected ferritin and nitric oxide synthase, which were up-regulated after 29 °C treatment.

Complementary DNAs were synthesized from 1 μ g of total RNA with 1 μ l Solaris RNA spike (Thermo-Scientific) using the qScript cDNA synthesis Kit (Quanta Biosciences), according to the manufacturer's instructions. Specific qRT-PCR primers (Table S6) were designed to amplify 100–200 bp PCR products. Assuming equal RNA loading, the Solaris spike controls are designed to act as a synthetic exogenous control to identify the presence of reaction inhibition thereby circumventing the need for a housekeeping gene^{40–42}. Spike-inoculated cDNA aliquots were diluted 1:10 and a 4 μ l sample was used in technical triplicates for 10 μ l qRT-PCR reactions including 0.5 μ l mix of forward and reverse primers, 5 μ l of GoTaq qPCR Master Mix (Promega), and 0.5 μ l of RNase free water, for 45 cycles. A melt curve analysis obtained by incubating the reactions for 10 s at 0.5 °C increments between 60 °C and 90 °C was generated for each pair of primers, to test for nonspecific amplification products. The comparative $\Delta\Delta$ Ct method was used, and fold changes were calculated using the $2^{-\Delta\Delta$ Ct} formula to estimate the relative amounts of transcripts in each sample⁴³. Ct refers to the cycle at which the fluorescence signal crosses the

threshold and by using the solaris spike control^{40–42} we normalized the expression to RNA loading. The MIQE guidelines were taken into account in designing real time profiles and analyzing their results⁴⁴.

Relative expression values for each gene and each biological replicate were calculated by the ratio of treatment relative expression over the average of control relative expression. The results of qPCR and RNA-seq fold change analyses are presented on a log₂ scale (Fig. S8). Our results show that there is a correlation between the RNA-seq and the qPCR results, based on log₂ fold gene expression (adjusted $r^2 = 0.86$; $p < 0.0001$). The fold changes calculated based on qRT-PCR were in the same direction and consistent with those in the RNA-seq data, thus confirming the RNA-seq results and validating our approach (Fig. S8).

Bioinformatic analysis. We utilized Partek Genomic suite software (version 6.6, Copyright©2012, Partek Inc., St. Louis, MO, USA) to plot a three-dimensional space principle component analysis and to generate Venn diagrams and hierarchical clustering heat maps for *S. pistillata* and *B. europaea* samples (Heat maps were generated using Euclidean distance as a similarity measure and average linkage). The fold changes were calculated for all contigs using the average of the relevant controls (each coral species by its control samples). An arbitrary cutoff of at least two fold (p -value < 0.05) was chosen to define a differentially expressed gene (DEG).

Functional gene analysis was done by David Bioinformatics Resources^{6,7,45,46} and KEGG pathway analysis via STRING 9.0 database⁴⁷, using the *Homo sapiens* orthologs annotations. Retrieving Gene Ontology (GO) biological processes (see core enriched GOs at Figs S2 and S3) enabled an enrichment analysis and analysis of the coral responses to long-term chronic stress.

We utilized a list of Cnidarian environmental stress genes⁴⁸ based on relevant literature to search the Swissprot and Uniprot 50 annotations. This indicated a differential expression between *S. pistillata* and *B. europaea* with respect to known Cnidarian environmental stress genes (Fig. S4) that corresponds to the results of the enrichment analysis.

References

- Hoegh-Guldberg, O. *et al.* Coral reefs under rapid climate change and ocean acidification. *Science* (80-). **318**, 1737–1742 (2007).
- Albright, R. *et al.* Reversal of ocean acidification enhances net coral reef calcification. *Nature* **531**, 362–365 (2016).
- Lejeune, C., Chevaldonné, P., Pergent-Martini, C., Boudouresque, C. F. & Pérez, T. Climate change effects on a miniature ocean: the highly diverse, highly impacted Mediterranean Sea. *Trends Ecol. Evol.* **25**, 250–60 (2010).
- Calvo, E. *et al.* Effects of climate change on Mediterranean marine ecosystems: the case of the Catalan Sea. *Clim. Res.* **50**, 1–29 (2011).
- Intergovernmental Panel on Climate Change (IPCC). Climate Change 2007: The Physical Science Basis. *Contrib. Work. Gr. I to Fourth Assess. Rep. Intergov. Panel Clim. Chang.* Ed. by S. Solomon *et al.* Cambridge Univ. Press, Cambridge, UK (2007).
- Garrabou, J. *et al.* Mass mortality in Northwestern Mediterranean rocky benthic communities: effects of the 2003 heat wave. *Glob. Chang. Biol.* **15**, 1090–1103 (2009).
- Israel national monitoring program, at the Gulf of Eilat, Scientific report, www.iui-eilat.ac.il (march 2002).
- Romano, S. L. & Palumbi, S. R. Evolution of Scleractinian corals inferred from molecular systematics. *Science* (80-). **271**, 640–642 (1996).
- Loya, Y. The Red Sea coral *Stylophora pistillata* is an r strategist. *Nature* **259**, 478–480 (1976).
- Maor-Landaw, K. *et al.* Gene expression profiles during short-term heat stress in the red sea coral *Stylophora pistillata*. *Glob. Chang. Biol.* **20**, 3026–3035 (2014).
- Goffredo, S., Mezzomonaco, L. & Zaccanti, F. Genetic differentiation among populations of the Mediterranean hermaphroditic brooding coral *Balanophyllia europaea* (Scleractinia: Dendrophylliidae). *Mar. Biol.* **145**, 1075–1083 (2004).
- Goffredo, S. *et al.* Inferred level of calcification decreases along an increasing temperature gradient in a Mediterranean endemic coral. *Limnol. Oceanogr.* **54**, 930–937 (2009).
- Caroselli, E. *et al.* Environmental implications of skeletal micro-density and porosity variation in two scleractinian corals. *Zoology* **114**, 255–264 (2011).
- Goffredo, S., Caroselli, E., Pignotti, E., Mattioli, G. & Zaccanti, F. Variation in biometry and population density of solitary corals with solar radiation and sea surface temperature in the Mediterranean Sea. *Mar. Biol.* **152**, 351–361 (2007).
- Goffredo, S. *et al.* Biomineralization control related to population density under ocean acidification. *Nat. Clim. Chang.* **4**, 593–597 (2014).
- Fantazzini, P. *et al.* Gains and losses of coral skeletal porosity changes with ocean acidification acclimation. *Nat. Commun.* **6**, 7785 (2015).
- Bhattacharya, D. *et al.* Comparative genomics explains the evolutionary success of reef-forming corals. *Elife* **5**, e13288 (2016).
- Karako-Lampert, S. *et al.* Transcriptome analysis of the scleractinian coral *Stylophora pistillata*. *PLoS One* **9**, e88615 (2014).
- Brown, B. E., Downs, C., Dunne, R. & Gibb, S. Exploring the basis of thermotolerance in the reef coral *Goniastrea aspera*. *Mar. Ecol. Prog. Ser.* **242**, 119–129 (2002).
- Fitt, W., Brown, B., Warner, M. & Dunne, R. Coral bleaching: interpretation of thermal tolerance limits and thermal thresholds in tropical corals. *Coral Reefs* **20**, 51–65 (2001).
- Császár, N. B. M., Ralph, P. J., Frankham, R., Berkelmans, R. & van Oppen, M. J. H. Estimating the potential for adaptation of corals to climate warming. *PLoS One* **5**, e9751 (2010).
- Kaniewska, P. *et al.* Major cellular and physiological impacts of ocean acidification on a reef building coral. *PLoS One* **7**, e34659 (2012).
- Kaniewska, P. *et al.* Transcriptomic changes in coral holobionts provide insights into physiological challenges of future climate and ocean change. *PLoS One* **10**, 1–30 (2015).
- Gates, R. D., Baghdasarian, G. & Muscatine, L. Temperature Stress Causes Host Cell Detachment in Symbiotic Cnidarians: Implications for Coral Bleaching. *Biol. Bull.* **182**, 324–332 (1992).
- DeSalvo, M. K. *et al.* Differential gene expression during thermal stress and bleaching in the Caribbean coral *Montastraea faveolata*. *Mol. Ecol.* **17**, 3952–71 (2008).
- de Castro, E. *et al.* ScanProsite: detection of PROSITE signature matches and ProRule-associated functional and structural residues in proteins. *Nucleic Acids Res.* **34**, W362–W365 (2006).
- Willander, H. *et al.* High-resolution structure of a BRICHOS domain and its implications for anti-amyloid chaperone activity on lung surfactant protein C. *Proc. Natl. Acad. Sci. US* **109**, 2325–9 (2012).
- Nerelius, C. *et al.* Mutations linked to interstitial lung disease can abrogate anti-amyloid function of prosurfactant protein C. *Biochem J* **416**, 201–209 (2008).
- Tasiemski, A. *et al.* Characterization and Function of the First Antibiotic Isolated from a Vent Organism: The Extremophile Metazoan *Alvinella pompejana*. *PLoS One* **9**, e95737 (2014).

30. Sievers, F. *et al.* Fast, scalable generation of high-quality protein multiple sequence alignments using Clustal Omega. *Mol. Syst. Biol.* **7**, 539 (2011).
31. Sanchez-Pulido, L., Devos, D. & Valencia, A. BRICHOS: a conserved domain in proteins associated with dementia, respiratory distress and cancer. *Trends Biochem. Sci.* **27**, 329–332 (2002).
32. Oliver, T. a. & Palumbi, S. R. Do fluctuating temperature environments elevate coral thermal tolerance? *Coral Reefs* **30**, 429–440 (2011).
33. Palumbi, S. R., Barshis, D. J. & Bay, R. A. Mechanisms of reef coral resistance to future climate change. *Science (80-)*. **14612**, 895–898 (2012).
34. Barshis, D. J. *et al.* Genomic basis for coral resilience to climate change. *Proc. Natl. Acad. Sci. USA* **110**, 1387–92 (2013).
35. Nevo, E. Evolution under environmental stress at macro- and microscales. *Genome Biol. Evol.* **3**, 1039–1052 (2011).
36. Hume, B. C. C. *et al.* Ancestral genetic diversity associated with the rapid spread of stress-tolerant coral symbionts in response to Holocene climate change. *Proc. Natl. Acad. Sci.* 201601910, doi: 10.1073/pnas.1601910113 (2016).
37. Levy, O. *et al.* Complex diel cycles of gene expression in coral-algal symbiosis. *Science* **331**, 175 (2011).
38. Grabherr, M. G. *et al.* Trinity: reconstructing a full-length transcriptome without a genome from RNA-Seq data. *Nat. Biotechnol.* **29**, 644–652 (2013).
39. Li, B. & Dewey, C. N. RSEM: accurate transcript quantification from RNA-Seq data with or without a reference genome. *BMC Bioinformatics* **12**, 323 (2011).
40. Mayfield, A. B., Hirst, M. B. & Gates, R. D. Gene expression normalization in a dual-compartment system: a real-time quantitative polymerase chain reaction protocol for symbiotic anthozoans. *Mol. Ecol. Resour.* **9**, 462–70 (2009).
41. Mayfield, A. B., Chan, P.-H., Putnam, H. M., Chen, C.-S. & Fan, T.-Y. The effects of a variable temperature regime on the physiology of the reef-building coral *Seriatopora hystrix*: results from a laboratory-based reciprocal transplant. *J. Exp. Biol.* **215**, 4183–4195 (2012).
42. Putnam, H. M., Mayfield, a. B., Fan, T. Y., Chen, C. S. & Gates, R. D. The physiological and molecular responses of larvae from the reef-building coral *Pocillopora damicornis* exposed to near-future increases in temperature and pCO₂. *Mar. Biol.* **160**, 2157–2173 (2013).
43. Livak, K. J. & Schmittgen, T. D. Analysis of relative gene expression data using real-time quantitative PCR and the 2-ddCT method. *Methods* **25**, 402–408 (2001).
44. Bustin, S. A. *et al.* The MIQE guidelines: minimum information for publication of quantitative real-time PCR experiments. *Clin. Chem.* **55**, 611–622 (2009).
45. Huang, D. W., Sherman, B. T. & Lempicki, R. A. Systematic and integrative analysis of large gene lists using DAVID bioinformatics resources. *Nat. Protoc.* **4**, 44–57 (2009).
46. Huang, D., Sherman, B. & Lempicki, R. Bioinformatics enrichment tools: paths toward the comprehensive functional analysis of large gene lists. *Nucleic Acids Res.* **37**, 1–13 (2009).
47. Szklarczyk, D. *et al.* The STRING database in 2011: functional interaction networks of proteins, globally integrated and scored. *Nucleic Acids Res.* **39**, D561–8 (2011).
48. Maor-Landaw, K. & Levy, O. In *The Cnidaria, past, present and future. The world of Medusa and her sisters* (eds. Goffredo, S. & Dubinsky, Z.) 523–543 (Springer, 2016).
49. Magie, C. R. & Martindale, M. Q. Cell-cell adhesion in the cnidaria: Insights into the evolution of tissue morphogenesis. *Biol. Bull.* **214**, 218–232 (2008).
50. D'Souza-Schorey, C. Disassembling adherens junctions: breaking up is hard to do. *Trends Cell Biol.* **15**, 19–26 (2005).
51. Nelson, W. J. & Nusse, R. Convergence of Wnt, b-Catenin, and Cadherin Pathways. *Science (80-)*. **303**, 1483–1488 (2004).

Acknowledgements

We thank Mr. M. Samuelson of the Faculty of Life Sciences, BIU, Israel for his help during this study. This study represents partial fulfillment of the requirements for a PhD thesis for K. Maor-Landaw at the Faculty of Life Sciences Bar-Ilan University, Israel. The research leading to these results has received funding from the European Research Council under the European Union's Seventh Framework Programme (FP7/2007–2013)/ERC grant agreement n [249930-CoralWarm: Corals and global warming: the Mediterranean versus the Red Sea]. Additional funding was provided to K. Maor-Landaw by the Mediterranean Sea Research Center of Israel. We also thank The Interuniversity Institute for Marine Sciences in Eilat (IUI) for support of this research.

Author Contributions

K.M.L., O.L., S.G., G.F. and Z.D. designed the research, K.M.L. performed the research, K.M.L., H.W.B., S.K.L. and M.S.D. analyzed the data, F.P., E.C., S.G. and O.L. supplied materials, K.M.L. and O.L. wrote the paper.

Additional Information

Supplementary information accompanies this paper at <http://www.nature.com/srep>

Competing financial interests: The authors declare no competing financial interests.

How to cite this article: Maor-Landaw, K. *et al.* Mediterranean versus Red sea corals facing climate change, a transcriptome analysis. *Sci. Rep.* **7**, 42405; doi: 10.1038/srep42405 (2017).

Publisher's note: Springer Nature remains neutral with regard to jurisdictional claims in published maps and institutional affiliations.



This work is licensed under a Creative Commons Attribution 4.0 International License. The images or other third party material in this article are included in the article's Creative Commons license, unless indicated otherwise in the credit line; if the material is not included under the Creative Commons license, users will need to obtain permission from the license holder to reproduce the material. To view a copy of this license, visit <http://creativecommons.org/licenses/by/4.0/>

© The Author(s) 2017